International Journal of Precision Engineering and Manufacturing-Green Technology
https://doi.org/10.1007/s40684-021-00399-4

Online ISSN 2198-0810
Print ISSN 2288-6206

REGULAR PAPER

Design Approach for Additive Manufacturing of a Dynamically Functioning System: Lifeboat Hook

Ulanbek Auyeskhan[1,2] · Namhun Kim[2] · Chung-Soo Kim[1] · Tran Van Loi[1,3] · Jihwan Choi[1] · Dong-Hyun Kim[1]

Received: 15 May 2021 / Revised: 13 September 2021 / Accepted: 3 October 2021

Abstract
The design freedom provided by Additive Manufacturing (AM) enables the part consolidation (PC) of sophisticated mechanical assemblies. However, PC has been mainly performed for static components in assemblies with nonmoving parts. In this regard, a new approach to assembly-level Design for Additive Manufacturing (A-DfAM) considering an industrial lifeboat hook assembly with a functionally dynamic system is proposed. The methodology comprises steps starting from inputting the Computer-Aided Design (CAD) files for the 3D printing of the final assembly and evaluation. Throughout the design stages, opportunistic and restrictive natures of DfAM within our methodology direct engineers and designers to manufacture optimized products. In addition, a comparative assessment of the original and final assemblies is also illustrated. Consequently, a significant part-count reduction after PC was achieved, and the prototype of the lifeboat hook components was printed via laser-powder bed fusion (L-PBF). This shows that by incorporating the suggested A-DfAM framework, it can serve as a potential guide to whoever intends to manufacture dynamic assemblies.

Keywords Part consolidation · Assembly-level DfAM · Finite element analysis (FEA) · Additive Manufacturing · Lifeboat hook

1 Introduction

Additive manufacturing (AM) has been paving an effective way in the field of prototype fabrication and flexible production with markedly different characteristics compared with conventional subtractive manufacturing such as drilling, milling, and cutting [1]. To apply AM, a systematic approach is adopted during overall design stages, normally referred to as Design for Additive Manufacturing (DfAM), offering); it offers a wide range of design freedom to provide sophisticated end-user parts as well as primitive components. A target design is possibly achieved via the inherent techniques of AM such as topology optimization [2], attaining a lightweight structure [3], and part consolidation [4]. In addition, the application of DfAM provides enhanced functions [5], reduces the weight of components, and requires less lead time [6].

Applying DfAM during a whole design stage can be classified as opportunistic and restrictive. While an opportunistic approach allows designers to come up with creative designs, the geometry is constrained owing to the 3D printing features in the case of restrictive DfAM [7]. Hence, when devising a new product with a higher design freedom, the former can produce AM-optimized output. In contrast, the latter is mostly utilized to replace conventional manufacturing via AM, conducted under the limitation of AM-specific features such as minimum thin wall thickness, overhangs, dimensional accuracy, surface finish, and other constraints associated with 3D-printing machines [8]. From a practical perspective, both opportunistic and restrictive DfAM should be utilized in conjunction to ensure design freedom and limitations, respectively. Thus, a notion of dual-DfAM which is a combination of opportunistic and restrictive DfAM, was first named in [7]. Dual-DfAM is a practical method that can be selected when

✉ Dong-Hyun Kim
dhk@kitech.re.kr

[1] 3D Printing Manufacturing Process Center, Korea Institute of Industrial Technology (KITECH), Ulsan, Republic of Korea

[2] Department of Mechanical Engineering, Ulsan National Institute of Science and Technology (UNIST), Ulsan, Republic of Korea

[3] Department of Mechanical Engineering, University of Ulsan, Ulsan, Republic of Korea

Published online: 11 November 2021

adopting AM instead of replacing with or optimizing for AM [9].

AM designing includes a particular feature to cover not only a component (C-DfAM) but also assembly-level products (A-DfAM) [7]. The C-DfAM predominantly focuses on improving the capabilities of individual components in contrast to the A-DfAM, which applies to an assembled system. A majority of DfAM studies have been discussed in C-DfAM while A-DfAM studies have been comparatively lagging [7] owing to their difficulty in deducing an optimized solution. The previous and current works of A-DfAM mainly deal with part consolidation (PC) to reduce the number of components in a mechanical assembly yet conserving original functionality or possibly presenting a better performance and a potential economic gain [10].

For the spread of AM technology, we need to consider a transition of DfAM applications from a static and component level to dynamic and assembly level, which effectively overcomes the high material and processing costs of AM. The demand for such dynamic assemblies using A-DfAM is also expected to considerably increase owing to the emergence of new transport means such as land or aerial vehicles. However, most of the consolidated assemblies are either nonmoving [11] or difficult to maintain at the time of use [12, 13] so far. It is, thus, an appropriate time to perform an in-depth study regarding a dynamic A-DfAM methodology while considering a significant factor such as product assembly complexity, which has a strong influence on assembly time [14].

As a case study for the dynamic A-DfAM framework, a lifeboat hook from Hyundai Lifeboat Co. Ltd. with a moving mechanism was chosen for the following merits: (1) it is mechanically operated to release a lifeboat from a mother ship; (2) a total of 74 parts including fasteners can provide a clear demonstration of PC; and (3) it is an attractive challenge to consider the heavy loading of more than 4 tons, applied to the hook, as a design rule of AM. During the DfAM process of the lifeboat hook, a new methodology was thoroughly utilized. It is an integration of A-DfAM and dual-DfAM for dynamic assemblies coupling with design validation through finite element analysis (FEA), product assembly complexity, and manufacturability by L-PBF. Consequently, our methodology incorporating input information, exploring new design space followed by validation will provide a systematic approach to a dynamic A-DfAM and new insight into a real industrial application of novel additive design.

2 Literature Review

2.1 Part Consolidation

PC is a potentially practical method that aids in reducing the number of overall components of a mechanical assembly and subsequently producing them via 3D printing processes, which become much simpler [15]. Since after PC assembling cost is no more relevant, the total piece price of a product can be reduced [10]. In addition, the supply chain of the subparts from various sources can be eliminated by printing the consolidated components. The US-based startup company, Relativity Space, claims that they can build up commercial space shuttle components completely through metal 3D printing. In addition, they reported that owing to the advances in AM, the number of parts can be reduced from 100,000 to only 1,000, and the overall manufacturing time is 10 times faster than that of a conventionally accepted aerospace industry benchmark [16]. Another notable example is a helicopter engine assembly consolidated by General Electric. The new consolidated design comprising 14 components is derived from 900 parts including fasteners [17]. Similarly, Schmelzle et al. [18] consolidated a hydraulic manifold comprised of 17 parts to 1 part, reducing the weight and height by 60% and 53%, respectively. These industrial products signify that PC is a strong design tool in A-DfAM.

However, the above-mentioned researchers either did not specify or provide a guide on how they consolidated the target assembly. They relied upon their expertise and did not discuss what guidelines were followed. In contrast, Yang and Zhao came up with a numerical approach for PC [19]. Considering the conventional Design for Assembly (DfA), they established a modified PC candidate detection algorithm with seven rules that could be applied for AM mechanical assemblies. They compared a manual and their proposed automatic implementation of PC in terms of time cost and showed how the method is relatively efficient. However, according to those authors, if there are single or multiple subassemblies, the manual intervention and implementation may perform better. In addition, an assignment of weighting strength between components based on the functional and physical interactions might be exhausting for an assembly with numerous components.

Kim and Moon provided PC by considering a functional flow (signal, material, and energy) [20] and assessing a product disassembly complexity at the last step of their proposed design method [21]. Their method is a well-established starting point though it bypasses the maintenance and AM-specific constraints for now. The previously mentioned two works are not intuitive for application and lack a clear case study with an illustration of an industrial dynamic assembly, respectively. Thus, there is a need for a simpler yet systematic approach to applying PC for A-DfAM, too.

Herein, the overview will be based on two specific methods of PC. First, a consolidated design in which the parts share common functions, i.e., functional integrity, is provided. Then, the PC is considered followed up by redesigning, namely structural optimization (topology optimization and lattice structure).

i) PC: functional integrity (FI)

The study conducted by Meisel et al. [22] illustrated the PC of a NASA pencil thruster assembly utilized in a rocket propulsion system. Originally, the thruster comprised of 12 parts machined from a Haynes 230 alloy that can endure an elevated temperature of 2000 °C and a pressure of around 19 bar. The AM design has eight components grouped in three main independent sections, namely, the nozzle, fuel injector, and oxidizer injector, each containing two or three components that share the same functionalities. This is to reduce the overall build height, which significantly affects the build time and cost of parts. In particular, within one assembly, it is better to circumvent designs with tall and short components in the same build chamber due to an excessive amount of powder to fill in. In addition, throughout the development process, they exploited a dual-DfAM at both the component and assembly level where appropriate. For example, in terms of the restrictive feature, it was mentioned that the build direction determined how to manufacture the axisymmetric internal channels. To avoid supports inside the thruster, which are difficult or impossible to remove, a self-supporting geometry was utilized; hence, the assembly was built parallel to a printer's build direction.

ii) PC: FI and redesigning

Yang et al. [23] performed PC according to FI accompanied with structural optimization. FI is based on two substeps, such as obtaining functional surfaces (FS) and the generation of functional volumes (FV) out of those surfaces. Usually, FS plays the role of boundary conditions disregarding manufacturing and assembly surfaces. Then, FV is created as a solid body interconnected by the extracted FS, and a heterogeneous lattice optimization can be performed on the generated FV. In the provided case study, the authors could reduce the total mass by around 20% and the part count from 19 to 7 based on the redesigning of the overall assembly and FI, respectively.

Another DfAM study conducted by Biswal et al. [24] shows the procedure of simplifying the Gantry Head assembly by incorporating topology optimization after PC. Similar to [24], the authors consolidated the main functional components and later performed topology optimization while maintaining the original stiffness of the consolidated parts. They could achieve part-count reduction from 9 to 2 and 32% weight reduction.

Based upon these methodologies, it was observed that there are no studies that considered PC of functionally dynamic assemblies experimentally validated by AM and product assembly complexity even though it is essential in providing a metric of how a conventionally manufactured design is improved by PC. Again, an integration of opportunistic and restrictive features of A-DfAM should also be considered throughout the design stages. In the next subsection, a brief background regarding product assembly complexity will be provided.

2.2 Product Assembly Complexity

Currently, automotive, aerospace, naval, medical, and many other industries heavily exploit mechanical assemblies such as pistons, engines, hydraulic pumps, and surgery devices [25]. In these industries, assembling is critical because around 50% of overhead is heavily correlated to the comprehensiveness and ease of assembly tasks such as handling and insertion based on DfA charts [26]. Thus, the complexity of the original assembly should be measured and could be reduced by PC.

To address complexity, one of the prominent studies in which ElMaraghy and Urbanic grouped complexity in the context of manufacturing systems into three varieties, namely, process, operational, and product complexities [27]. It was earlier mentioned that there is no process complexity in AM for parts within the same bounding box while complexity increases in the case of traditional manufacturing processes; hence, no information regarding the same is provided in this work.

Operational complexity is related more to the human factor; every operator has different capabilities, experience, and skills within the manufacturing environment [28, 29]; thus, complexity assessment should be performed systematically before any essential decisions are made. However, this type of complexity is not in the scope of the current study because it can be suggested as a part of cognitive ergonomics [29] during 3D printing.

The third category, product complexity, more specifically product assembly complexity is our main concern, which deals with the material, design, and specifications of the individual components within an assembly. Such complexity is used to assess to what extent the assembling of a particular product is difficult considering assembling operations. To quantify product assembly complexity, DfA analysis of handling and insertion attributes both in manual and automatic assembling are first extracted based on every component of a product. Then, the model for product assembly complexity, $C_{product}$, in Eq. (1), originating from Shannon's Information theory [30], is used in terms of product assembly index $CI_{product}$, the number of parts and fasteners. Herein, the product assembly complexity is an essential validation metric to carefully assess the design change before and after PC.

$$C_{product} = \left[\frac{n_p}{N_p} + CI_{product}\right]\left[\log_2(N_p + 1)\right] + \left[\frac{n_s}{N_s}\right]\left[\log_2(N_s + 1)\right] \tag{1}$$

Here, N_p is the total number of parts. N_s is the total number of fasteners. n_p is the number of nonrepeating unique

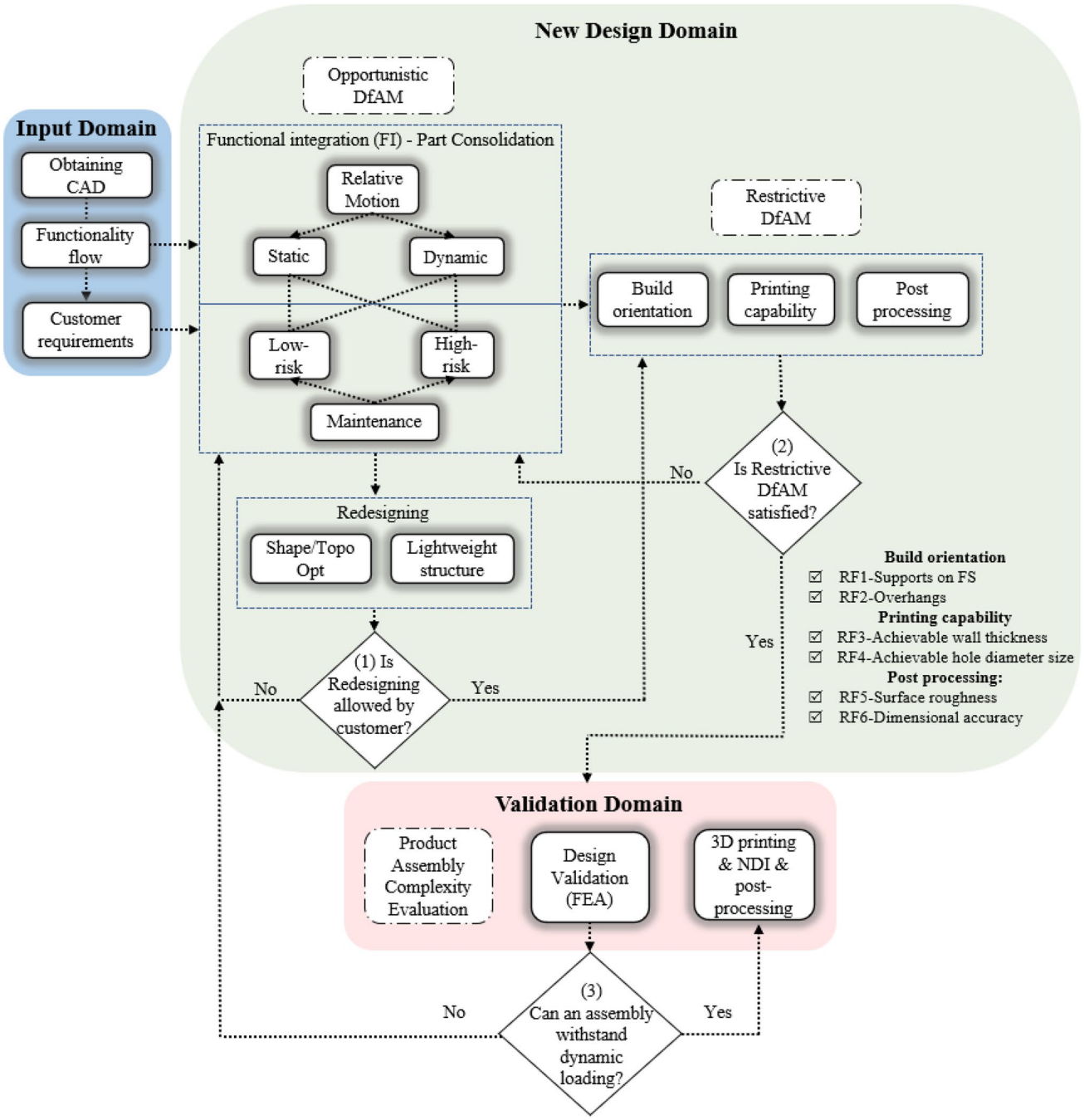

Fig. 1 A systematic A-DfAM framework for dynamic assemblies involving input domain, new design domain and validation domain. NDI stands for non-destructive inspection

parts. n_s is the number of nonrepeating unique fasteners. $C_{product}$ is the product assembly complexity.

Moreover, it should be mentioned that the handling and insertion metrics vary in manual and automatic assembly. Thus, a reader can refer to [28] for a detailed procedure.

3 Methodology

Figure 1 shows the A-DfAM framework with the application of opportunistic and restrictive natures of DfAM (dual-DfAM) considering product assembly complexity, FEA, and printability of assembly components in this work. The

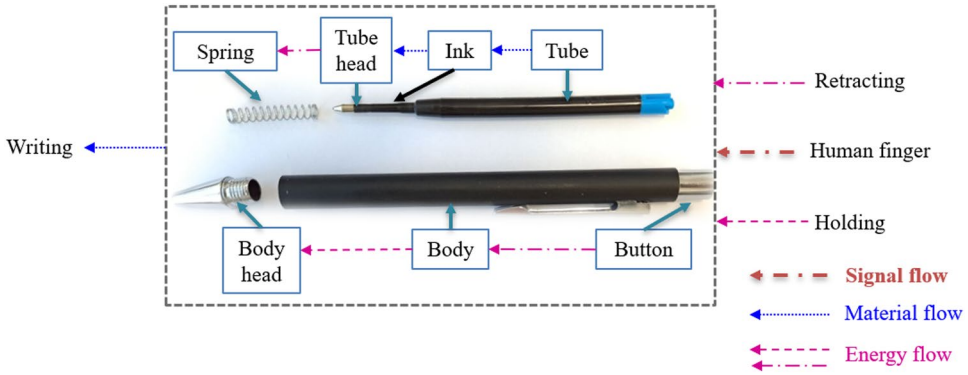

Fig. 2 A functionality flow chart of a ballpen

methodology is divided into the input, new design, and validation domains.

3.1 Input Domain

At the outset, the input information such as CAD files, customer needs, and functional requirements are obtained. The customer needs in product design vary based on a specific discipline and an industry [31]. For example, the customer needs for the assemblies involve (1) functionality; (2) assemblability; (3) durability; (4) maintenance frequency; and (5) structural integrity. After identifying customer needs, functionality flow is generated by following signal, energy, and material flows [20]. These three flows can be regarded as transmitted information describing the purpose of each member in a closed system. For easier understanding, in Fig. 2, a ballpen activated by a human (signal) which has retracting, holding (energy), and finally writing (material) functions is shown. Each component has specific functions connected with other parts in the ballpen. In the same manner, an illustration of functionality flow can be obtained for any mechanical assemblies. Even though a retrieval of the functionality chart of a system with numerous parts and fasteners (e.g., > 100) would be an arduous job, dividing it into subassemblies (i.e., modules) might potentially mitigate the issue [32].

3.2 New Design Domain

Next, a new design domain through the lenses of opportunistic and restrictive DfAM is explored. According to the functionality flow, modularized groups that share the same functionalities are distinguished. In particular, the static and dynamic parts are grouped into separate modules as shown in Fig. 1. According to the heuristic rules such as those of relative motion (do other parts move relative to the target component?), maintenance (is a part feasible for maintenance upon assembling), and material variance (should the consolidating parts be composed of different materials?), [15] we can obtain preliminary consolidated designs. Applying only these rules are not enough to finalize the design of an assembly. As it was emphasized in [33], specific manufacturing and lifecycle constraints must also be considered. Thus , after applying these rules, a resultant design should undergo restrictive facets of DfAM. In the devised A-DfAM framework, the components are assumed to have the same materials within the PC stage; hence, the material variance rule is not adopted.

Based on the relative motion rule, modules can be split into static and dynamic groups, and then those components are classified as low- and high-risk-failure parts as provided by customers, see Table 1. In this study, low-risk parts are the ones that need less frequent maintenance, i.e., monthly/annually. Conversely, the parts that are maintained daily/weekly are assigned as high-risk parts. Later, by performing PC on low-risk parts, a possibility of redesigning is assessed based on customer requirements. For instance, if a target assembly is a part of a bigger system and should be assembled within a designated space, a variation (e.g., designing thicker, bigger parts targets than the original) in the final design is limited pertaining to the assemblability. If a customer requirement does not allow redesigning a target assembly, then PC will be performed without further redesigning. This decision making is shown as (1) in Fig. 1. The next stage is an implementation of restrictive DfAM for the assemblies that passed only the FI or redesigning steps. The condition for qualifying the restrictive DfAM stage is noted as (2) in Fig. 1.

The restrictive facets are considered such as build orientation, printing capability, and post processing. The criteria in each of the cases are summarized in Table 2 such as restrictive facet (RF1-6). Notably, these criteria are characteristic to an in-house SLM printer. Based on RF1, it is best to avoid supports on the critical FS (SFFS) because after removal residual, materials are left that caused dimensional instability and rough surfaces, particularly in the areas where postprocessing is difficult. Additionally, RF1 and the other RF2-6 are largely affected by common factors, such as Z-height, support area, support volume, and XY-section.

Table 1 A-DfAM sheet for dynamic assemblies

Parts	Modules	Opportunistic DfAM						Restrictive DfAM					$C_{product}$ (Δ%)
		Part consolidation				Redesigning		Build orientation		Printing capability		Post processing	
		Relative motion		Maintenance		Shape/Topo optm	Lightweight structure	RF1	RF2	RF3	RF4	RF5	RF6
		Static	Dynamic	Low-risk	High-risk								
A	Module-1												
B													
C													

Reducing Z-height results in less build time, the other two factors result in less support and reduced residual stress, respectively. After considering these features, if PC-ed components are strictly confined and do not satisfy set criteria (i.e., less build time and less supports on FS) the PC stage might need to be revisited. Moreover, the details regarding an economic compensation between employing PC and resultant build orientations with supports on FS amount will be investigated in future work.

There are various types of commercially available support generation software, though most of them do not provide multi-objective optimization: Z-height, support area, support volume, and XY-section)—all considered simultaneously by allowing a user to semi-automate the procedure. That may be a challenge for designers new to AM owing to a lack of experience with 3D printers. An attempt to automatically optimize build orientation was extensively reported by Zhang [34], though it still needs human involvement at certain points for selecting the desired properties. Thus, automatic extraction of FS based on the assembly mechanism and the subsequent generation of a reasonable amount of supports on those FS is also suggested as a potential avenue for future research.

3.3 Validation Domain

Following PC, manual or automatic assembly attributes such as handling and inserting should be evaluated using a DfA chart. Upon filling in the chart, the part assembly complexity, C_{part}, is calculated as follows:

$$C_{part} = \frac{C_h \sum_1^J C_{h,f} + C_i \sum_1^K C_{i,f}}{\sum_1^J C_{h,f} + \sum_1^K C_{i,f}} \tag{2}$$

where C_h *(handling)* and C_i *(inserting)* are the complexity factors, and J and K are the number of attributes in handling and inserting, respectively. Then, by calculating the x_p, which is a percentage of the nonrepeating unique parts in the assembly with n components, the product complexity index, $CI_{product}$, is easily obtained:

$$CI_{product} = \sum_{p=1}^{n} x_p C_{part} \tag{3}$$

By substituting Eqs. (3) into (1), the product assembly complexity $C_{product}$ can be determined [28]. Notably, this metric is a potential tool for analyzing a change in designs (Δ%) between conventional and PC-ed modules. Care should be taken when applying $C_{product}$ in the assemblies wherein redesigning is possible. This is because those cases also involve topologically optimized and lightweight structures (i.e., mass reduction).

Table 2 Restrictive Facets Characteristic to a L-PBF machine (Germany, SLM company SLM280HL) was used in this work

Group	Code	Restrictive feature	Definition	Parameter
Build orientation	RF1	SFFS	Support fraction on functional surfaces (FS)	< 25% of overall FS area
	RF2	Overhangs	Downskin areas without support	< 43°
Printing capability	RF3	Achievable wall thickness	Minimum feature size that can be printed	≥ 0.2 mm
	RF4	Achievable hole diameter	Maximum circular hole diameter printed in Z-direction achievable without support	< 8 mm
Post processing	RF5	Surface roughness	Surface roughness after removing support structures	Accessibility of supports to be removed and (R_a < 10 µm)
	RF6	Dimensional accuracy	After printing the part, less intervention of machining	± 50 µm

SFFS can be varied upon the application area in our case we set 25% this is reflected in Sect. 7 in detail

Later design validation by FEA should be performed considering the stress responses of every PC-ed module in an assembly. Following FEA, if there is a module with plastic deformation, PC should be reconsidered. At the last stages, experimental validation through 3D printing, postprocessing, and inspection of the PC-ed design is performed

4 Case Study—Lifeboat Hook

A lifeboat hook with a safe working load (SWL) of 4 tons containing 74 parts including fasteners from Hyundai Lifeboat (HLB) Co. Ltd. was selected, as shown in Fig. 3. This case study illustrated the reduction in the number of components of the dynamic system. Originally, there were two hooks distanced according to company regulations, as shown in Fig. 3a. The hook assembly must endure a weight of 25–41 people based on lifeboat models. There is a main body comprising an upper plate welded to two side plates, as shown in Fig. 3b. All other components are assembled upon these main structural plates. In Fig. 3c, an initial state of the hook suspended by a closed self-locker with the main chain link is depicted. In addition, a description of the lifeboat hook's moving mechanism is provided in Fig. 3d. After the release cable is pulled by an operator, the cam and stopper instantaneously release from the hook body.

4.1 Functionality Flow Generation

In the early design stage, a functionality flow and customer requirements were acquired. The functionality flow including energy (loading), signal flows, and a structural connection was obtained, as shown in Fig. 4. Accordingly, the clusters or modular groups (cam, stopper, hook, self-locker, and pendent lug) were identified, and subsequently neighborhood parts that share the same functions such as releasing from lever (cam), transferring motion to the hook part (stopper), and carrying the hook for fixation or maintenance (pendent lug) are highlighted. Furthermore, maintenance should be performed weekly and monthly for high- and low-risk parts, respectively, to avoid any potential accidents in the sea, according to the HLB company. Either lattice or topology optimization is challenging on the plates or other components because the system undergoes a heavy loading in multiple directions, implying that the thickness of the plates (8 mm) must be increased. However, a lifeboat wall is manufactured with a fixed slot (i.e., 8.3 ± 0.2 mm) for installations of the side plates aimed to reduce vibration during operation. Thus, redesigning techniques for this particular design space are not recommended.

4.2 Part Consolidation of the Lifeboat Hook Assembly

The hook assembly can be explicitly grouped into two systems such as static (structural) and dynamic components. The dynamic modular groups include the cam, stopper, hook, self-locker, and pendent lug. The other group includes the structural plates group that serves as the backbone of the assembly. Because the cam, stopper, self-locker, and hook groups require frequent maintenance, the PC of the respective components should be performed carefully. For example, the very first part that makes the system move is the cam. From the cam group, indicators from both sides of the plates can be consolidated with bushes independently from each other, as shown in Fig. 5a,b. The pendent lug was consolidated with only bush because it is not a high-risk failure component; however, it should not be printed already assembled to the plates as a complete replacement would be required then even in the case of small defects. The stopper, self-locker, and hook groups along with the cam itself are classified as high-risk owing to the frequently required inspections. Finally, all other parts that are not subjected to movement are accommodated at the consolidated plates.

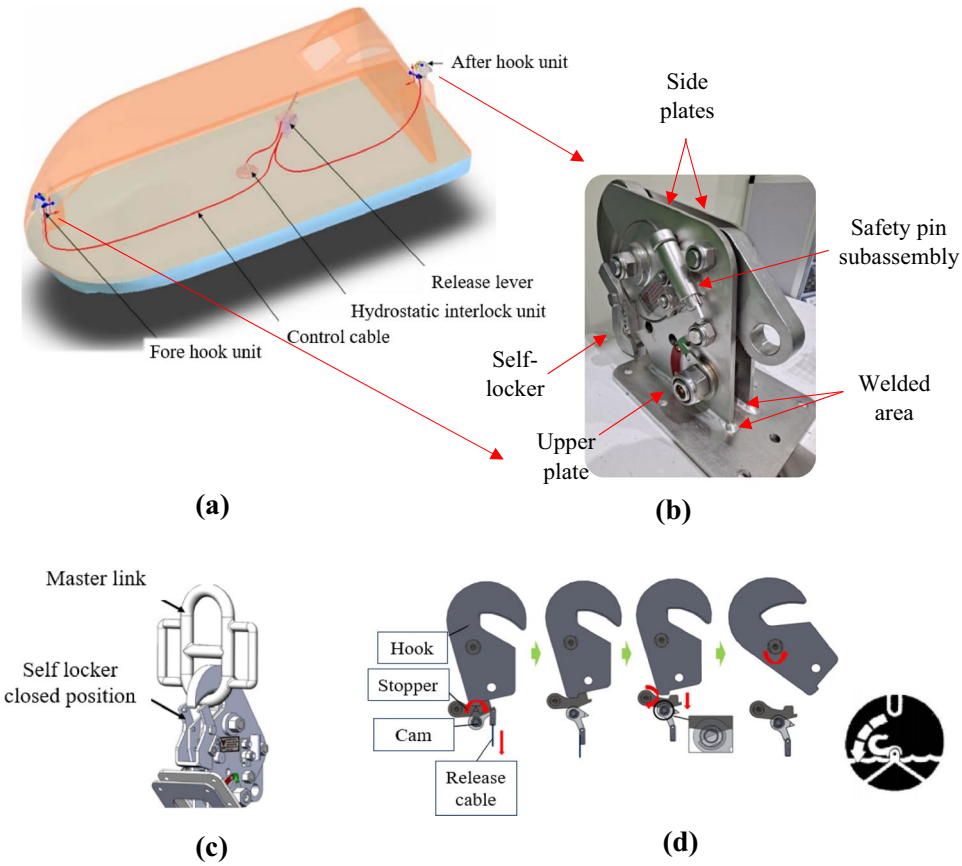

Fig. 3 **a** Conventional lifeboat model with a release gear system, **b** hook assembly, **c** closed position of hook by self-locker along with suspending link, **d** release mechanism. Initially, the cable is released then the cam lets the stopper rotate and sets the hook free

Note that redesigning for this particular assembly is not performed following customer requirements.

4.3 Implementation of Restrictive DfAM

The next step is to consider restrictive DfAM. Primarily, the factors causing the need for restrictive DfAM are minimizing build height, support surface area, support volume, and XY-section. For example, in the case of PC-ed plates, the resultant values of the main factors related to five possible orientations are shown in Table 3. Except for O-4, which was oriented manually, the other placements are automatically generated via Magics Software based on the main factors mentioned above. O-1 and O-2 have a minimum build height of 51.219 mm and the least support surface of 454.905 mm^2. In both cases, SFFS is 0%; however, these alignments make postprocessing very laborious because of excess support between the plates, as shown in Fig. 6. In addition, support volumes of O-1 and O-2 are almost 3–4 times more than that of O-3, O-4, and O-5. In O-3, the maximum XY-section is the least among the rest; however, it has the highest SFFS (23.84%) and build height (200.695 mm). The last orientations, O-4 and O-5 possess SFFS of 23.33% and 0.37%, respectively. At first sight, O-5 might seem more favorable because of the smaller SFFS; however, the Z-height of O-5 is 2.24 times higher than that of O-4, which increases the build time. Moreover, in the case of O-5, there are support volumes in difficult-to-reach places. Therefore, O-4 was chosen for experimental validation; the respective A-DfAM design sheet is provided in Table 4.

Before diving into FEA validation, one should proceed to the $C_{product}$ evaluation step. In this case study, a manual assembly was chosen because the assembling process is not automated for the lifeboat hook. Detailed results and discussion are presented in Sect. 6.1.

5 FEA Setup

5.1 Material Selection

The certification, inspection, and maintenance of this hook assembly were rigorously conducted; thus, there should not be any damage related to both the mechanism and structural components. In this regard, the AM tool steel 1.2709 which has a superior yield strength was utilized. It has 2.2 and 4.0 times larger yield strength than the base materials of duplex steel and SUS304L, respectively, though AM tool steel is more prone to corrosion in a seawater environment [35].

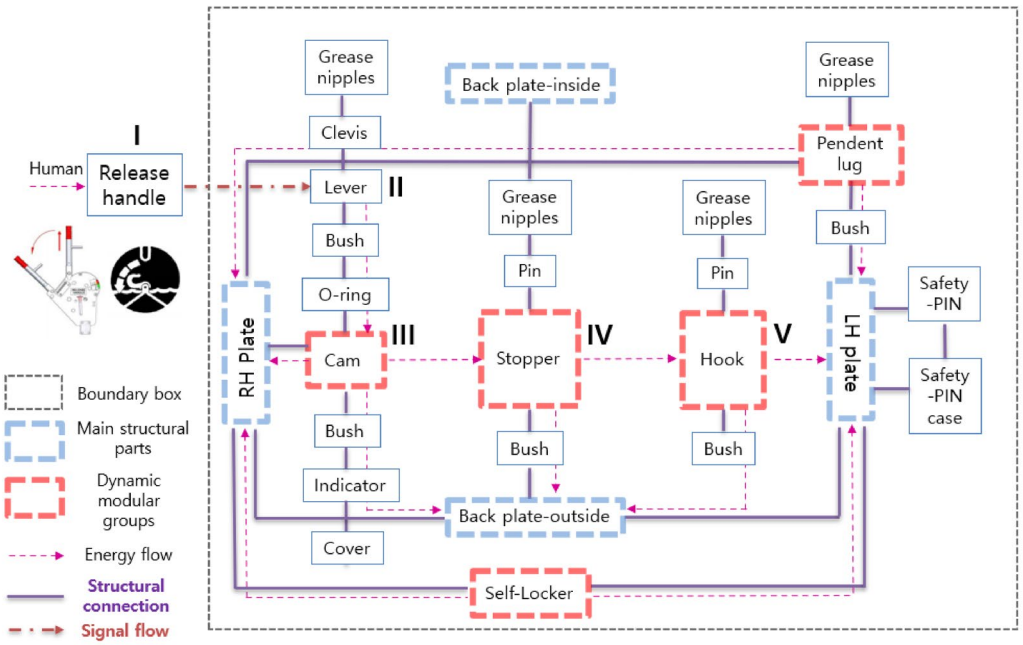

Modular group	Cam	Stopper	Hook	Self-Locker	Pendent lug
Function	i) Initiates dynamics of the assembly ii) Releases stopper	i) Inhibits random movement ii) Releases the hook part	i) Lifting the dynamic loading ii) Releases from the chain link	i) Locks the chain link at the hook	i) Provides safe handling of the assembly
Location	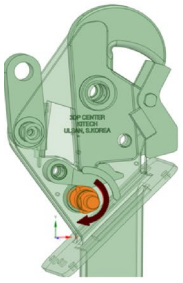	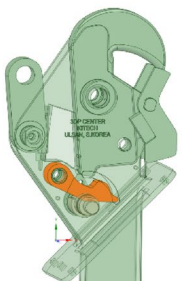	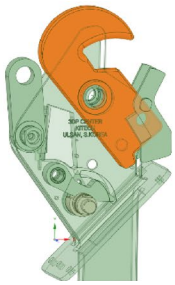	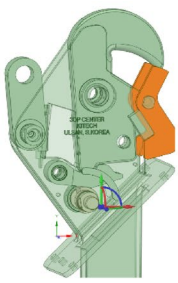	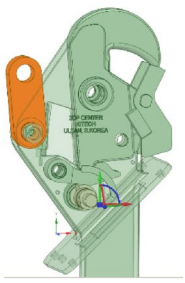

Fig. 4 Functional flow of the hook assembly. Steps (I–V) indicate a dynamic movement of release handle (I), lever (II)-cam (III), stopper (IV) and hook (V) consecutively. It should be noted that dynamic groups (except self-locker due to maintenance) such as cam, stopper, hook and pendent lug force their members to move simultaneously because they are connected structurally. For example, after the release handle is operated, the lever makes the whole cam group rotate and transfers the motion to the stopper group and afterward to the hook group subsequently releasing from the chain link

This factor was overlooked for now because in later stages, a corrosion-resistant coating can be applied on the surface of the 3D-printed hook parts. Other material properties are listed in Tables S1 and S2.

5.2 Boundary Conditions

This hook assembly could be installed on different types of conventional lifeboats; hence, information on the maximum weight capacity (with 41 people) was imported from the company to ensure safety. The target SWL is 4 tons with fixed supports and finally set up at the lifeboat wall. In summary, the boundary conditions for the hook assembly were constrained as follows in Fig. 7.

(A) Full weight = 41 people + equipment = 32,750 N/hook.
(B) SWL = 4 t.
(C) Fixed supports.
(D) Lifeboat wall.

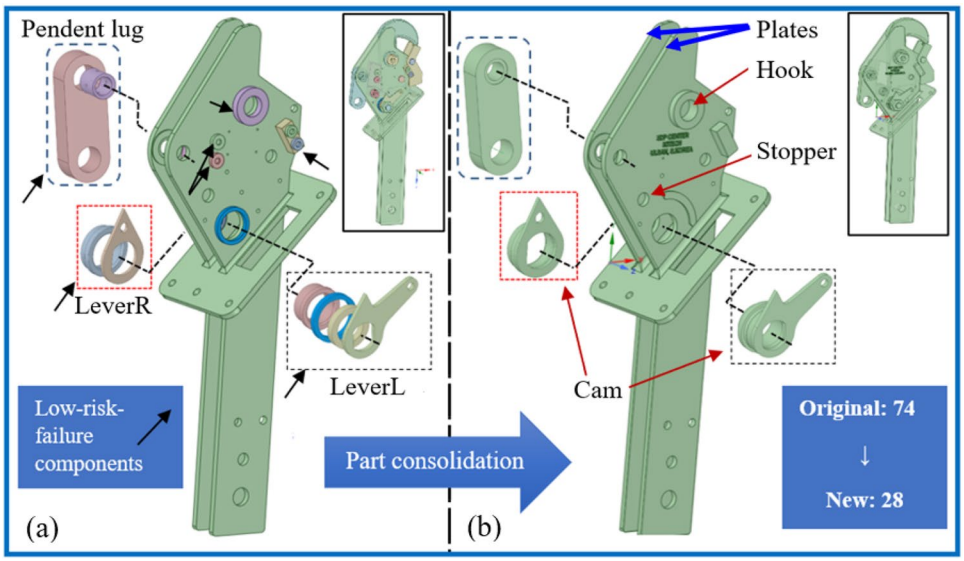

Fig. 5 **a** Original design. **b** Design after PC. In both images, cam, stopper and hook parts (locations are shown by red arrows) are hidden because they do not accommodate any of the parts due to the frequent maintenance and possible high risks. The same outlined colors represent the respective consolidated components

6 Results and Discussion

6.1 Product Assembly Complexity Analysis

Table 5 shows that product assembly complexity from the original to a new design has substantially decreased by 26.01%. The main reason behind this is the fewer parts (43%) and fasteners (81%), overall from 74 to 28, indicating less handling and insertion operations. The next one is to avoid welding within the assembling process, which requires more assistance by holding down the plates. As mentioned above, the side and upper plates must be kept aligned during welding in the original design while they could be simply consolidated at the outset of A-DfAM and printed as illustrated in Sect. 7. Moreover, it should be highlighted that the complexity assessment does not involve postprocessing in the case of AM though this might need to be included in future studies within handling attributes of product assembly complexity because the same PC-ed component with different build orientations and FS can yield more complexity.

6.2 Dynamic and Static Heavy Loadings

Originally, before releasing from the suspension cables, the hook undergoes a sudden loading. If the hook stays without moving at that instant, the dynamic loading would be considerably more severe than the static loading equivalently applied in a quasistatic manner. Moreover, it is possible to relate them with the help of a dynamic amplification factor (DAF) [36]. Because the computational engineering time is expensive to simulate the dynamics of the whole assembly movement, instead a static situation was employed at the various instants of times along with the varying angle of the hook after release. Thus, the results of the equivalent stresses of different assembly parts from individual cases (A–E) in Fig. 8 can be multiplied by the DAF.

Table 3 Comparison of five orientations of downscaled hook plates in terms of Z-height, support surface, max XY-section

	Units	O-1	O-2	O-3	O-4	O-5
Z-height	mm	51.219	139.492	200.695	70.236	157.461
Support surface	mm^2	12133.716	198.975	805.242	1757.188	219.954
Max XY-section	mm^2	6283.113	776.712	454.905	959.648	616.135
Support volume	mm^3	44195.876	36769.748	11084.898	10083.864	12072.660
Support on FS	%	0	0	23.840	23.330	0.370

Except for O-4, four of placements are automatically produced based on min Z-height, less support surface, less max XY-section, min support volume and a SFFS via Magics Software. O-4 was positioned manually to (1) avoid excess support between plates, (2) minimize support volume and (3) mitigate support generation on FS at the same time. A thorough explanation of positioning and experimental demonstration is provided in Sect. 7

6.3 Dynamic Amplification Factor

In practice, the hook assembly vibrates owing to the rough sea waves, resulting in a damped system. To compensate for this, Giurgiutiu's statement in which DAF would be lower than 2 in the system where damping was applied can be relied upon [36]. This is because vibration would decrease before reaching its maximum amplitude. In addition, Maglute et al. reported that tensions in suspension cables for a lifeboat upon dynamic loading are 1.5 times the static case [37]. The weight of their lifeboat system significantly outweighs the lifeboat in this work. Therefore, based on the above-mentioned works, dynamic and static heavy loadings in a lifeboat hook assembly can be related using Eq. (4):

$$DHL = DAF \cdot SHL = 1.5 \cdot SHL \tag{4}$$

where, DHL and SHL are dynamic and static heavy loadings for the lifeboat hook, respectively.

The Von Mises stress values times DAF of hook and plates in the original and new designs at different scenarios are displayed in Fig. 9 because they experience a bigger portion of the loading after releasing from the cables. There is little difference between AM and conventional designs owing to employing the same materials as explained in Section S1.

In addition, Von Mises stress should be determined under SWL at specific angles. A case is provided wherein the loading has vector components. Namely, one of the criteria that should be considered under the Life Saving Appliances Code is 100% of SWL (= 4 tons) at an angle of 20° to the vertical axis [38]. In addition, the hook is expected to be suspended with a full loading of boarding people and released accordingly. After the release, there should not be any damage. The resultant equivalent stresses of the essential components, i.e., hook and plates, were defined as shown in Fig. 10.

Notably, the Von-Mises stresses of the hook and plates shown in Fig. 9 are large enough to cause permanent deformation. In practice, the suspending cables that hold the lifeboat hook are released at a speed of 5 knots = 2.57 m/s upon the loading exerted by both a lifeboat with full equipment and SWL. Thus, there is not enough time to fully allocate the loadings because the hook slides rapidly. Even in an accidental scenario in which hook movement is locked at a certain angle. AM tool steel properties can still withstand a large amount of loading without causing structural damage to the lifeboat walls. Finally, experimental validation via 3D printing the PC-ed lifeboat hook assembly will be provided in the next section.

7 Experimental Validation

For 3D printing, tool steel 1.2709 feedstock was employed because of the single material nature of the SLM280HL twin-laser metal printer. In addition, the consolidated design was downscaled by three times to ensure fitting in the build chamber (285 · 285 · 360 mm) of the printer. Metal L-PBF was selected to demonstrate the printability of the PC-ed hook assembly.

Next, care must be taken due to the restrictive DfAM features, as mentioned in Sect. 3.1. For example, when there is a long part to be printed along the recoater path, it is better to minimize the XY area at every slice by tilting a part to a certain angle to avoid residual stresses and possible contact with the recoater as shown in Fig. 11.

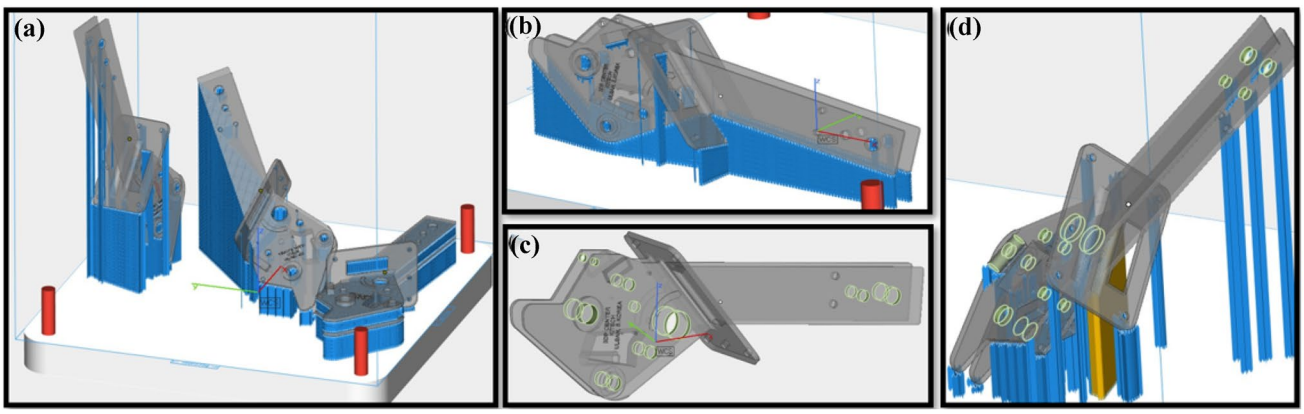

Fig. 6 **a** C-plate orientations listed in Tables 2, O-1, O-2 and O-3 (from right to left), **b** manually aligned O-4, **c** highlighted FS (in green) and **d** O-5 with marked FS. Except for O-4, all fail to consider easy postprocessing even though they optimize the orientation of PC-ed c-plate in terms of build height, less support area, maximum XY-section and less FS. All the above-mentioned factors should satisfy

Table 4 A-DfAM sheet for lifeboat hook assembly

Parts	Modules	Opportunistic DfAM						Restrictive DfAM						$C_{product}$ (Δ%)
		Part consolidation				Redesigning		Build Orientation		Printing capability		Post processing		
		Relative Motion		Maintenance		Shape/ Topo optm	Lightweight structure	RF1	RF2	RF3	RF4	RF5	RF6	
		Static	Dynamic	Low-risk	High-risk									
Side plate-L	Plates group	Y		Y		N	N	Y	Y	Y	Y	Y	Y	6.948 (26.01 %)
Side plate-R				Y										
Upper plate				Y										
Block				Y										
Safety pin				Y										
Support-plates				Y										
Support-self-locker				Y										
Lever	Cam group- Lever-L		Y	Y		N	N	Y	Y	Y	Y	Y	Y	
Spacer				Y										
Bush-L				Y										
Clevis				Y										
Support				Y										
Indicator	Cam group- Lever-R		Y	Y		N	N	Y	Y	Y	Y	Y	Y	
Bush-R				Y										
Pendent lug	Pendent group		Y	Y		N	N	Y	Y	Y	Y	Y	Y	
Bush				Y										

For example, the cam group is dynamic with low-risk components except for the cam (main part) because it needs periodic maintenance. Then, the cam group is divided into right- and left-side submodules to ensure easy access to assemble and each submodule was subsequently PC-ed. Regarding restrictive DfAM, support on FS in the case of O-4 is less than 25% along with appropriate alignment for removal of supports. At last product assembly complexity of the original design was evaluated and as a result decreased by one-fourth. Parts that need frequent maintenance (e.g., cam) are listed as high-risk and hence not shown in the table (Y-yes, N-no)

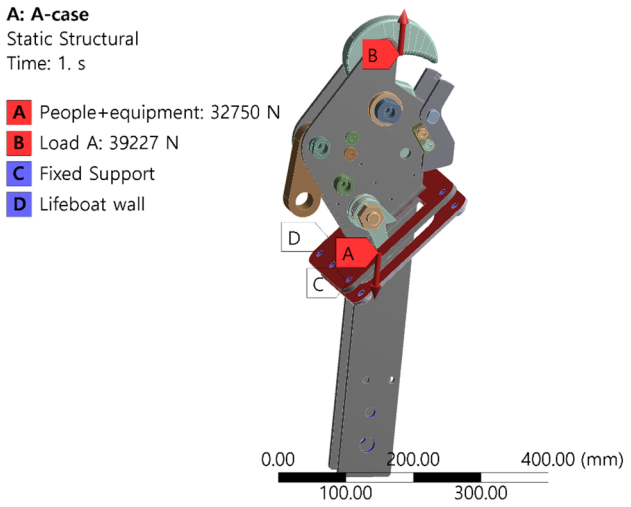

Fig. 7 Boundary conditions of the hook assembly for FEA. Maximum capacity of a lifeboat is 41 people thus the maximum weight is applied in the boundary conditions. A and B are loadings while C is fixed supports at the holes colored in purple. D is also a fixed support representing a lifeboat wall between upper and bottom plates

Furthermore, if some of the parts printed with supports horizontally can roughen an FS, positioning those parts along the Z-axis is preferred.

Usually, the overhang angle should not exceed 45° in the 3D printing process [39]; however, in terms of printer specifications, it is adjustable by ± 2°; hence, herein, 43° was used by considering the tool steel nature under a powerful laser. Then, the minimum diameter of the supportless holes can be considered, some of which are FS printed in the Z-axis specific to the 3D printer and material type. The work performed in [40] mentions that the authors could print circular holes composed of the same tool steel without supports in the range of 0.5–10 mm. However, the upper bound of the holes' diameter here is limited to 8 mm to ensure there are no significant sagging, burned areas, and cavities (Fig. 12).

It is a usual practice for the parts that have a flat surface without any complex projection facing onto the platform, volume supports 2–3 mm above the build platform are used. The projected supports can reduce the volume by ~ 50% than that in the case of using manually removable supports. Because wire cutting is not suitable for sophisticated geometries, customized band-saw-removable supports with heights of 5 mm were generated using AM build preparation software Magics v. 23.01.

Even though there are parts manually aligned and tilted efficiently, as shown in Fig. 6; Table 3, note that automatic support generation in the software often might not face the specific needs of the complex parts. For example, in Fig. 13, the offset values are needed because of the overridden supports, which makes it laborious to remove after printing. The support areas, S_1 and S_2, were initially mutually inclusive but later separated, as shown in Fig. 13a. However, when applying offset values for overhang supports, the tilted angle of supports should be lower than that of the overhang angle, 43°. In this manner, these supports can be modified to provide a balance between employing minimum support and overhangs.

After configuring supports and orientations of the parts shown in Fig. 13b, process parameters suggested by the SLM solutions were assigned as shown in Table 6 based on Eq. (5).

$$E(\textit{Energy density}) = \frac{P}{v \cdot h \cdot t}\left(\frac{J}{mm^3}\right) \tag{5}$$

Finally, all consolidated hook assembly components were printed within 11 h, as presented in Fig. 14. After printing, the parts were extracted without heat treatment as they were only meant for a prototype. Furthermore, the representative c-plates were 3D-scanned with a brief analysis provided in Figures S3 and S4.

8 Conclusions

A new A-DfAM that covers the workflow starting with an early design stage up until the experimental validation of the dynamically functioning assembly was proposed in this work. A detailed assessment considering opportunistic and restrictive facets of DfAM, namely PC and 3D-printing specific constraints were examined, respectively. As a case study, the real lifeboat hook assembly from Hyundai Lifeboat Co. Ltd. was chosen. In addition, product assembly complexity analysis demonstrated how the conventional design was improved. The contributions from our A-DfAM methodology can be listed as follows.

- A real industrial product with a moving mechanism and numerous components was optimized.
- A comprehensive FEA approach within the AM context.
- Demonstration of PC via a functionality flowchart for a dynamic system.
- Experimental validation of a complex designed structure.

Table 5 Reduction in the number of components and comparison of product assembly complexities

Assembly	Number of parts	Number of fasteners	$C_{product}$
Original hook	37	37	9.391
AM hook	21	7	6.948

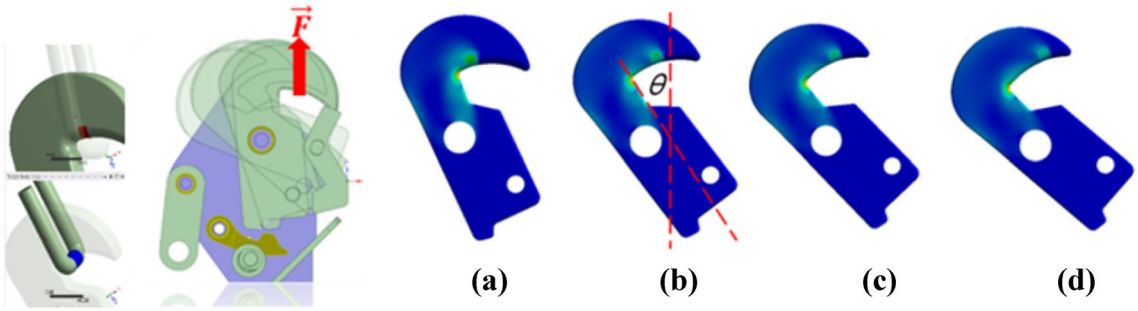

Fig. 8 Hook part after release from the suspension cable

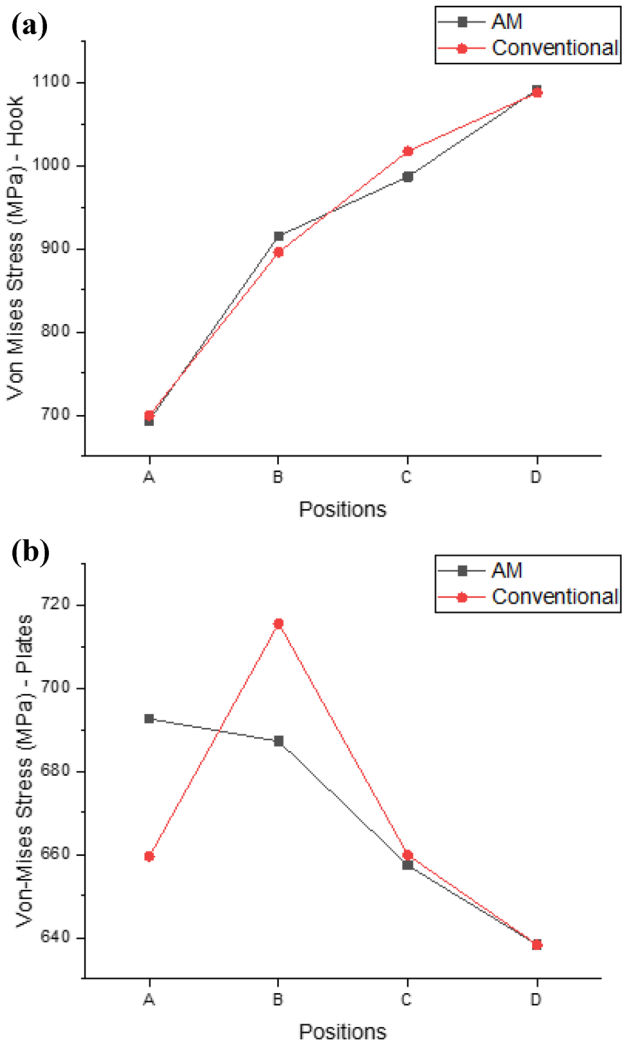

Fig. 9 Maximum Von Mises Stress (in MPa) of hook (**a**) and plates (**b**) in case of AM vs. conventional designs. A representative sensitivity analysis is provided in Fig. S2

This work within the presented A-DfAM framework attempted to perform PC on the lifeboat hook assembly resulting in 46 fewer components than the original design, which significantly challenges the traditional manufacturing industries. Even though the optimization steps of the prototype on a smaller scale are available, current rapid advances in AM promises practitioners to be able to progress in realistic bigger dimensions.

Because the proposed methodology was aimed only for the application of L-PBF printers, the developed method should be modified according to the characteristics of other type printers, for example, such as binder jetting (BJ) and stereolithography (SLA). In addition, it is assumed that a material variance rule is not applied in this work as a single-material printer can also be utilized to demonstrate the proposed framework. While this rule is crucial for assemblies with different materials, the assumption is justifiable based on the current availability of multi-material printers, which print similar to a single-material printer.

Moreover, for future studies, there is still room for developing computerized assessment of assembly complexity based on DfA and automatic FS generation of dynamic systems within the PC context. The main motivation behind this relies upon having computational tools to rapidly analyze whole dynamic mechanical assemblies that have hundreds or thousands of components. Additionally, a multi-objective optimization based on build orientations and support volume to minimize manufacturing cost and time will be studied in future works.

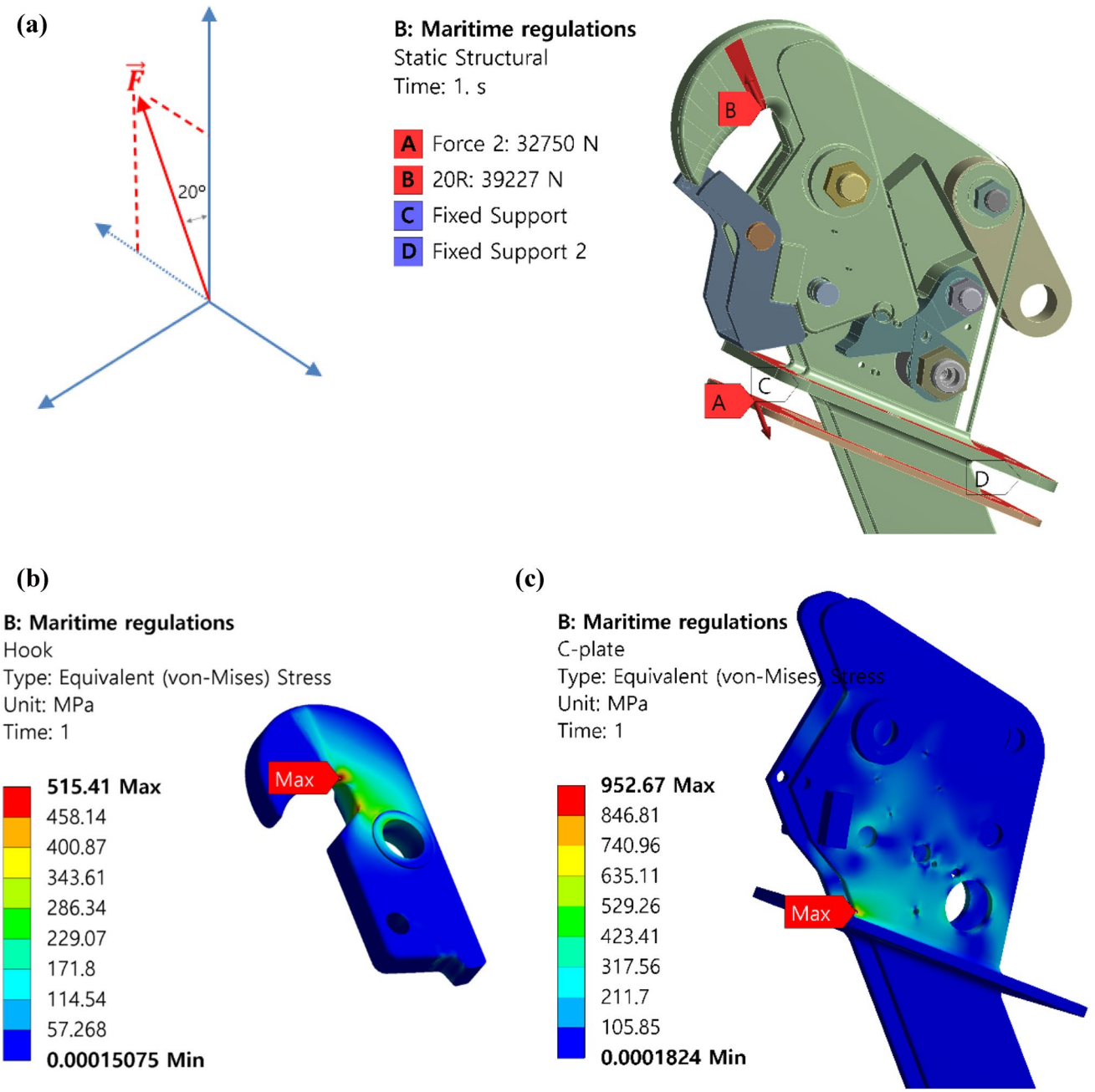

Fig. 10 **a** Boundary conditions at an angle of 20°. **b** Von Mises stress of hook and **c** c-plate under SWL at an angle of 20° with stress concentration labeled as max. C and D are fixed supports at the holes and between two plates, respectively

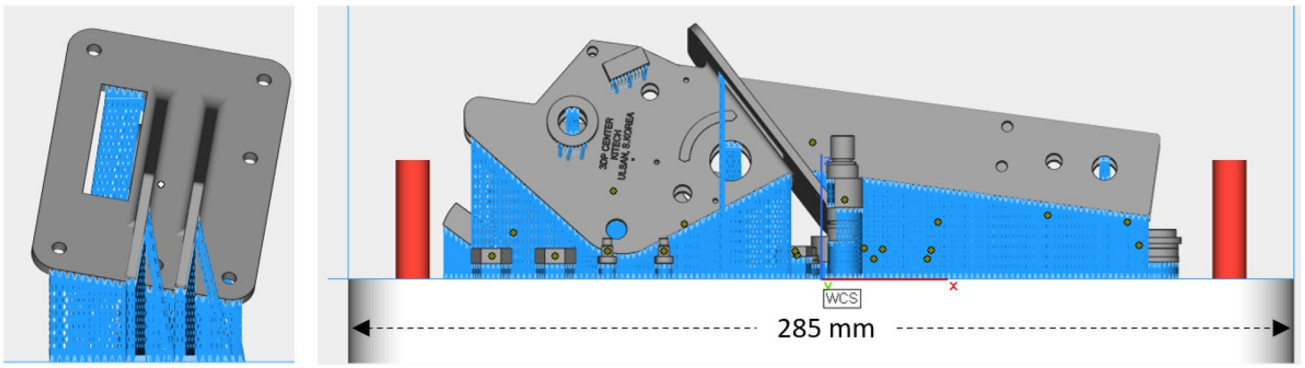

Fig. 11 A tilted c-plate along the recoater path with a side view

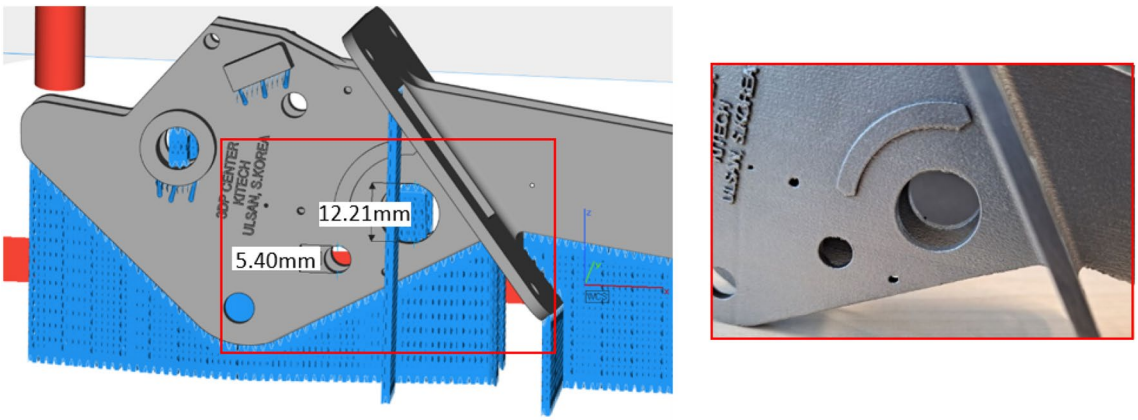

Fig. 12 FS (holes) with and without supports illustrated with actual printed c-plate

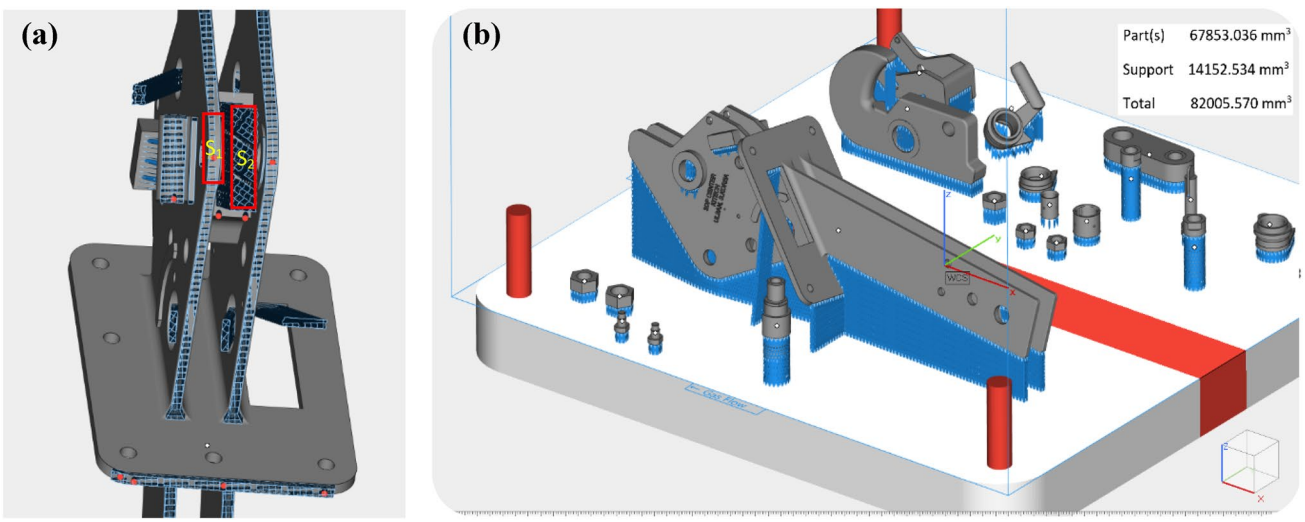

Fig. 13 **a** Splitting overridden supports, **b** support configuration of all the components

Table 6 Laser parameters to print a downscaled hookassembly

Laser power (W)	Hatch distance (μm)	Speed (mm/s)	Layer thickness (μm)
200	100	850	50

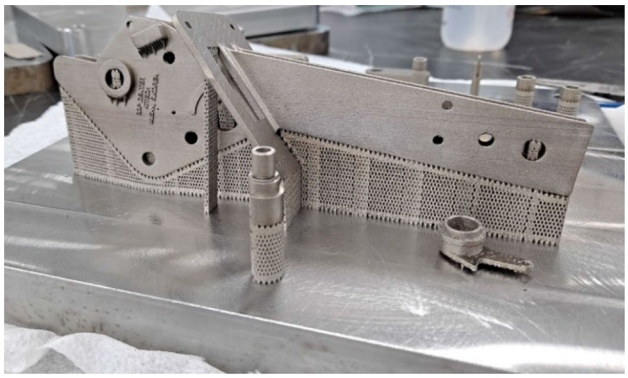

Fig. 14 Downscaled SLM-ed hook parts

Supplementary Information The online version contains supplementary material available at https://doi.org/10.1007/s40684-021-00399-4.

References

1. Diegel, O., Schutte, J., Ferreira, A., & Chan, Y. L. (2020). Design for additive manufacturing process for a lightweight hydraulic manifold. *Additive Manufacturing*, 36, 101446
2. Gebisa, A. W., & Lemu, H. G. (2017). A case study on topology optimized design for additive manufacturing. *IOP Conference Series Materials Science and Engineering., 276*(1), 012026.
3. Wang, P., Song, J., Nai, M. L. S., & Wei, J. (2020). Experimental analysis of additively manufactured component and design guidelines for lightweight structures: A case study using electron beam melting. *Additive Manufacturing*, 33, 101088
4. Liu, J. (2016). Guidelines for AM part consolidation. *Virtual and Physical Prototyping*, 11(2), 133–141
5. Reichardt, A., Shapiro, A. A., Otis, R., Dillon, R. P., Borgonia, J. P., McEnerney, B. W., et al. (2020). Advances in additive manufacturing of metal-based functionally graded materials. *International Materials Reviews, 66,* 1–29.
6. Kim, D. H., Lee, J., Bae, J., Park, S., Choi, J., Lee, J. H., et al. (2018). Mechanical analysis of ceramic/polymer composite with mesh-type lightweight design using binder-jet 3D printing. *Materials, 11*(10), 1941.
7. Laverne, F., Segonds, F., Anwer, N., & Le Coq, M. (2015). Assembly based methods to support product innovation in design for additive manufacturing: An exploratory case study. *Journal of Mechanical Design, Transactions of the ASME*, 137(12), 1–8
8. Simpson, T. W. (2018). *Manufacturing for Design. Not the Other Way Around*. https://www.mmsonline.com/columns/manufacturing-for-design-not-the-other-way-around
9. Dordlofva, C. (2020). A design for qualification framework for the development of additive manufacturing components-a case study from the space industry. *Aerospace*, 7 (3), 25
10. Knofius, N., Van Der Heijden, M. C., & Zijm, W. H. M. (2019). Consolidating spare parts for asset maintenance with additive manufacturing. *International Journal of Production Economics*, 208, 269–280
11. Reiher, T., Lindemann, C., Jahnke, U., Deppe, G., & Koch, R. (2017). Holistic approach for industrializing AM technology: from part selection to test and verification. *Progress in Additive Manufacturing*, 2(1–2), 43–55
12. Cuellar, J. S., Smit, G., Plettenburg, D., & Zadpoor, A. (2018). Additive manufacturing of non-assembly mechanisms. *Additive Manufacturing*, 21, 150–158
13. 3D printing moving parts fully assembled—28-Geared Cube: 3 Steps—instructables. https://www.instructables.com/3D-printing-moving-parts-28-Geared-Cube/. Accessed 8 Oct 2020
14. Boothroyd, G., & Alting, L. (1992). Design for assembly and disassembly. *CIRP Annals Manufacturing Technology, 41*(2), 625–636.
15. Boothroyd, G., Dewhurst, P., & Knight, W. (2002). *Product design for manufacture and assembly*. CRC Press.
16. Sertoglu, K. (2020). Relativity space secures California facility to produce first fully 3D printed rocket—3D printing industry. https://3dprintingindustry.com/news/relativity-space-secures-california-facility-to-produce-first-fully-3d-printed-rocket-168750/. Accessed 8 Oct 2020
17. Kellner, T. (2020). An epiphany of disruption: GE additive chief explains how 3D printing will upend manufacturing | GE News). https://www.ge.com/news/reports/epiphany-disruption-ge-additive-chief-explains-3d-printing-will-upend-manufacturing. Accessed 8 Oct 2020
18. Schmelzle, J., Kline, E. V., Dickman, C. J., Reutzel, E. W., Jones, G., & Simpson, T. W. (2015). (Re)Designing for part consolidation: Understanding the challenges of metal additive manufacturing. *Journal of Mechanical Design, Transactions of the ASME, 137*(11), 1–12.
19. Yang, S., Santoro, F., & Zhao, Y. F. (2018). Towards a numerical approach of finding candidates for additive manufacturing-enabled part consolidation. *Journal of Mechanical Design Transactions of the ASME, 140*(4), 041701.
20. Saldana, C. (2019) Design Functions and Solutions, Woodruff School of Mechanical Engineering, Georgia Institute of Technology. http://2110.me.gatech.edu/sites/default/files/documents/Lecture_Slides/me2110_spring_2019_lecture_05_functionssolutions.pdf
21. Kim, S., & Moon, S. K. (2020). A part consolidation design method for additive manufacturing based on product disassembly complexity. *Applied Sciences, 10*(3), 1100.
22. Meisel, N. A., Woods, M. R., Simpson, T. W., & Dickman, C. J. (2017). Redesigning a reaction control thruster for metal-based additive manufacturing: A case study in design for additive manufacturing. *Journal of Mechanical Design, Transactions of the ASME*, 139(10), 1–8
23. Yang, S., Tang, Y., & Zhao, Y. F. (2015). A new part consolidation method to embrace the design freedom of additive manufacturing. *Journal of Manufacturing Processes*, 20, 444–449
24. Biswal, R., Venkatesh, V., & Arumaikkannu, G. (2020). Investigation on part consolidation for additive manufacturing with SIMP method. *Materials Today Proceedings*, 46(10), 4954–4961
25. Whitney, D. E. (2004). *Mechanical assemblies: Their design, manufacture, and role in product development* (Vol. 1). Oxford University Press.
26. Swift, K. G., & Booker, J. D. (2013). Assembly costing. *Manufacturing process selection handbook* (pp. 393–409). Elsevier.
27. ElMaraghy, W. H., & Urbanic, R. J. (2003). Modelling of manufacturing systems complexity. *CIRP Annals Manufacturing Technology, 52*(1), 363–366.

28. ElMaraghy, W. H., & Urbanic, R. J. (2004). Assessment of manufacturing operational complexity. *CIRP Annals Manufacturing Technology, 53*(1), 401–406.
29. Mattsson, S. (2013). What is perceived as complex in final assembly?—to define, measure and manage production complexity. p. 145. https://core.ac.uk/download/pdf/70601735.pdf
30. Shannon, C. E., & Weaver, W. (1949). *The mathematical theory of communication*. University of Illinois Press.
31. Khalid, H. M., & Helander, M. G. (2004). A framework for affective customer needs in product design. *Theoretical Issues in Ergonomics Science*, 5(1), 27–42
32. Hölttä-Otto, K., & de Weck, O. (2007). Degree of modularity in engineering systems and products with technical and business constraints. *Concurrent Engineering Research and Applications*, 15(2), 113–125
33. Fagade, A. A., & Kazmer, D. (1993). Optimal Component Consolidation in Molded Product Design, ASME Paper No. DETC1999/DFM-8921
34. Zhang, X., Le, X., Panotopoulou, A., Whiting, E., & Wang, C. C. L. (2015). Perceptual models of preference in 3D printing direction. *ACM Transactions on Graphics*, 34(6), 1–12
35. Ansell, T. Y., Ricks, J. P., Park, C., Tipper, C. S., & Luhrs, C. C. (2020). Mechanical properties of 3D-printed maraging steel induced by environmental exposure. *Metals*, 10(2), 1–11
36. Giurgiutiu, V. (2008). Structural Health Monitoring, p. 50
37. Magluta, C., Roitman, N., & Batista, R. C. (1996). Dynamic behaviour analysis of a lifeboat system under simulated accidents. *Mechanical Systems and Signal Processing*, 10(6), 763–774
38. IMO revised recommendation on testing of life-saving appliances.
39. Thomas, D. (2009). The development of design rules for selective laser melting the development of design rules for selective laser melting, p. 25
40. Milan, D., Ivana, Z., Pavel, H., & Ondrej, H. (2017). Accuracy of holes created by 3d printing (dmls). In: Annals of DAAAM and proceedings of the international DAAAM symposium, pp. 467–473

Ulanbek Auyeskhan is a graduate student at Ulsan National Institute of Science and Technology. At the same time, he is a student researcher at Korea Institute of Industrial Technology in 3D Printing Manufacturing Process Center, Ulsan. His main direction of research activity is Design for Additive Manufacturing involving both simulation and experiments. His current research interests include optimization of industrial components by application of additive design rules and design theory.

Namhun Kim received his Ph.D. in Industrial and Manufacturing Engineering from Penn State University, University Park, PA, USA in 2010. He earned his BSc in 1998 and MSc in 2000 from KAIST. After that, he worked as a senior researcher in Samsung Corning for five years (from 2000 to 2005). He joined UNIST in 2010 and is currently a professor in the Department of Mechanical Engineering, acting as the director of Advanced Additive Manufacturing Research Center at UNIST, Korea. His scientific interests include design for additive manufacturing in future mobility systems, manufacturing system modeling and agent-based simulation.

Chung-Soo Kim received his Ph.D in mechanical and aerospace engineering from Seoul National University in 2013. In September 2013 he joined Research Laboratory ofElectronics at Massachusetts Institute of Technology and continued his research on a single nano-digit nanofabrication and non-demolition quantum electron microscope. In November 2017 he joined Global Technology Center at Samsung Electronics and worked for advanced manufacturing technologies and digital transformation. In November 2019 he joined Korea Institute of Industrial Technology and currently working on design for manufacturing, additive manufacturing and advanced manufacturing technologies based on electron, ion, and photon beam technologies at various length-scale.

Tran Van Loi received a B.S. in mechatronics engineering from Hanoi University of Science and Technology, Ha Noi, Viet Nam. He is currently a student in a combined course (M.S. and Ph.D.) at School of Mechanical Engineering, University of Ulsan, Ulsan, South Korea. He has been working as a research student at 3D Printing Manufacturing Process Center, Korea Institute of Industrial Technology (KITECH), Ulsan, South Korea. His research focus is on lightweight structure, cooling systems, and metal 3D printing.

Jihwan Choi is a researcher currently working at the Korea Institute of Industrial Technology, 3D printing Manufacturing Process Center. He graduated from the Department of Mechanical Engineering at Ulsan University. His main activities include 3D printing, 3D scanner operation and research application development.

Dong-Hyun Kim received his Ph. D degree about computational materials science in Materials and Science and Engineering at University of Florida. He worked at Ames Laboratory in Iowa, US as a postdoctoral researcher for one year, and later carried out process and device simulation related with mechanical stress at semiconductor division of Samsung Electronics for 4 years. Now he is a director of 3D Printing Manufacturing Process Center in Ulsan, Republic of Korea, and also studied FEM analysis and Addtive Manufacturing at Korea Institute of Industrial Technology. His main research is oriented towards simulation-based DFAM and its experimental validation.